

STATUS OF SUPERCONDUCTING ELECTRON LINAC DRIVER FOR RARE ION BEAM PRODUCTION AT TRIUMF

R.E Laxdal, F. Ames, R.A. Baartman, I. Bylinskii, Y.C. Chao, D. Dale, K. Fong, E. Guetre, P. Kolb, S.R. Koscielniak, A. Koveshnikov, M. Laverty, Y. Ma, M. Marchetto, L. Meringa, A.K. Mitra, N. Muller, R. Nagimov, T. Planche, W.R. Rawnsley, V.A. Verzilov, Z. Yao, Q. Zheng, V. Zvyagintsev, TRIUMF, Vancouver

Abstract

A MW class cw superconducting electron linac is being installed at TRIUMF as a driver for radioactive beam production through photo-fission. The ARIEL e-linac will house five 1.3GHz nine-cell cavities in three cryomodules and accelerate up to 10mA of electrons to 50MeV. A first phase of installation will see three cavities in two cryomodules installed by the end of 2014. The injector cryomodule has been installed with cryogenic, rf and beam acceleration tests completed. The second cryomodule is installed and being prepared for first tests. The linac status is reported.

INTRODUCTION

The ARIEL project [1] will allow a three-fold increase in the RIB delivery hours for the existing ISAC I & II experimental facilities. In brief the project consists of augmenting the present 500MeV (50kW) proton driver beam from the cyclotron and associated ISAC target stations with the addition of a new electron linac driver of 50MeV (0.5MW) and a second 500MeV (50kW) proton beam driver from the cyclotron and associated two new target stations and low energy RIB delivery systems. A first stage of the ARIEL installation including a 30MeV portion of the e-Linac and electron beamlines plus new ARIEL building and infrastructure is now nearing completion. The second phase encompassing the upgrade of the e-Linac to full energy, new target stations new proton beamline and low energy RIB beamlines is now under fund request adjudication.

Accelerated electrons can be used to generate RIBs via the photo-fission process [2]. The electrons are slowed either in the target material itself or in an upstream converter material to generate bremsstrahlung photons that produce fission in the actinide target material. The fission production resonance is centered near an incident photon energy of 15 MeV such that the production yield saturates around an electron energy of 50MeV. A beam current of 10mA at 50MeV is required to produce the goal rates of 10^{13} fissions/sec in an actinide target of sufficient density. This sets the operating boundary envelope for the completed electron linac.

The electron linac is housed in a pre-existing shielded experimental hall adjacent to the TRIUMF 500MeV cyclotron that has been re-purposed as an accelerator vault. The e-linac is being installed in a staged way with stages shown schematically in Fig. 1.

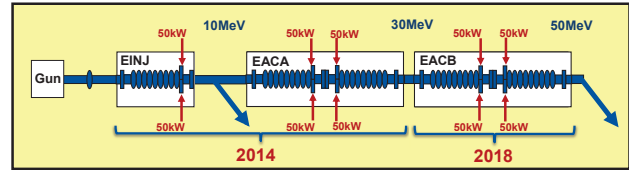


Figure 1: The stages of the e-Linac project.

A first phase consisting of a 300kV 16mA electron gun, an injector cryomodule, ICM, containing one 1.3GHz nine-cell cavity and an accelerating cryomodule, ACM1, containing two 1.3GHz nine-cell cavities plus associated beamlines is now installed and is in various stages of commissioning. This first phase is designed to accelerate cw up to 10mA of electrons at 30MeV but the initial beam dumps and production targets will only be compatible with 100kW operation. A second phase, dependent on funding, will see the addition of a second accelerating module and a ramp up in beam intensity to the full 50MeV 0.5MW capability.

ARIEL E-LINAC DESIGN

An rf frequency of 1.3GHz is chosen to take advantage of the considerable global design effort at this frequency both for pulsed machines (ILC) but also for cw ERL applications [KEK, Cornell, BerlinPro]. The linac architecture was determined by the choice of final cw beam power and the available commercial cw rf couplers at the design rf frequency of 1.3GHz. The CPI produced coupler developed with Cornell for the ERL injector cryomodule is capable of operation at 50kW cw. The cavity design allows two CPI couplers per cavity arranged symmetrically around one end delivering a total of 100kW of beam loaded power. This sets a maximum gradient per cavity at 10MV/m. A total of five cavities are required to reach 50MeV and 0.5MW beam power. It is our intention to install a future ERL ring with injection and extraction between 5-10MeV and so a single cavity off-line injector cryomodule was chosen plus two 2-cavity accelerating modules. The electron hall is shown in Fig. 2 as it would appear at the end of Phase II.

Electron Gun

The electron source [3] provides electron bunches with charge up to 15.4 pC at a repetition frequency of 650 MHz. The main components of the source are a gridded dispenser cathode in a SF₆ filled vessel, and an in-air high

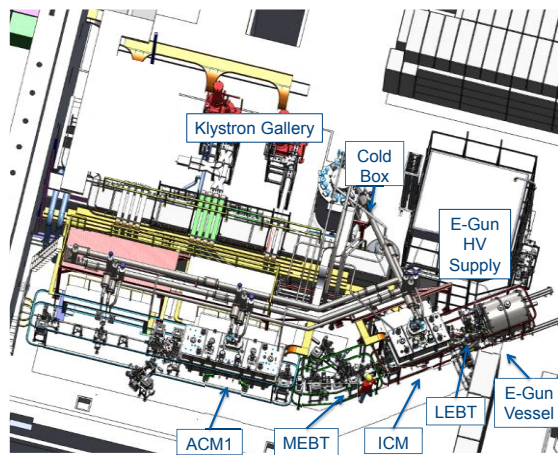


Figure 2: The phase I configuration of the e-linac.

voltage power supply. The beam is bunched by superimposing a RF modulation to overcome a DC suppression voltage on the grid. Unique features of the gun are its cathode/anode geometry to reduce field emission and transmission of RF modulation via a dielectric (ceramic) waveguide through the SF6. The latter obviates the need for a HV platform inside the vessel to carry the RF generator and results in a significantly smaller/simpler vessel. An impedance network inside an HV shroud matches the waveguide to the cathode.

Cavities

The cavity parameters include $f=1.3e9$, $L=1.038m$, $R/Q=1000$, $E_a=10MV/m$. For $Q_o=1e10$ the cavity power is $P_{cav}=10W$. A rendering of the jacketed cavity is shown in Fig. 3.

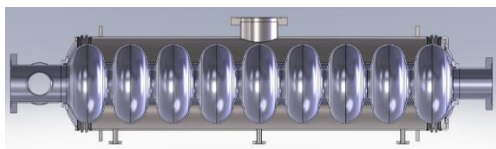


Figure 3: The e-Linac nine cell cavity with jacket.

The inner cells take their shape from the Tesla nine cell cavities but the end groups are modified to accept the two power couplers and to help push HOMs to dampers located on each end. On the power coupler end there is a stainless steel damping tube coaxial with the beam tube and extending into the beam tube by 17mm. On the opposite end of the cavity a coaxial CESIC tube is used [4]. Each tube is thermally anchored at 77K and thermally isolated from the cavity by a thin walled stainless steel bellows. The dampers are sufficient to reduce the HOMs to meet the BBU criterion of $R_d/Q*Q_L < 1e6$. The beam tube diameters on the coupler end and opposite end are 96mm and 78mm respectively. The vacuum jacket is made from Ti with a bellows on either end. A single 90mm diameter chimney allows for large cw rf loads of up to 60W per cavity assuming a conservative heat transfer of 1W/cm².

Cryomodules

The ACM module is shown in Fig. 4.

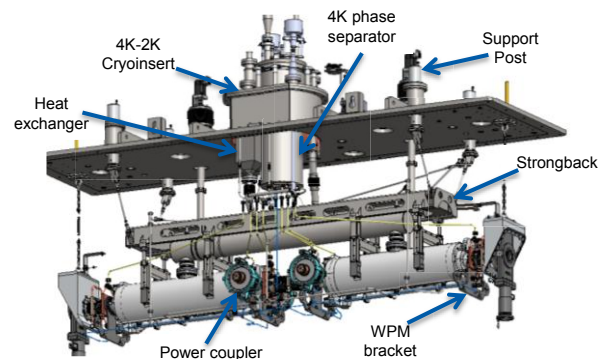


Figure 4: Accelerating cryomodule for ARIEL e-Linac.

The cryomodule design has been reported elsewhere [5]. In brief the module is a top-loading box-like structure with a stainless steel vacuum chamber. The cold mass is suspended from the lid and includes a stainless steel strongback, a 2K phase separator pipe, cavity support posts and the cavity hermetic unit. The hermetic unit consists of the niobium cavities, the end assemblies, an inter-cavity transition (ICT) with a stainless steel HOM damper, the power couplers (FPC) and an rf pick-up. The end assemblies include the warm-cold transition (WCT), CESIC HOM damping tubes and beam-line isolation valves. Other features include a scissor jack tuner and warm motor, LN2 cooled thermal isolation box and two layers of mu metal and alignment monitoring via a WPM diagnostic system.

Each cryomodule is outfitted with an on-board 4K to 2K cryogenics insert. The insert consists of a 4K phase separator, a 2.5gm/sec heat exchanger and a JT expansion valve, a 4K cooldown valve and a 4K thermal intercept syphon supply and return. During cooldown the 4K valve is used to direct LHe to the bottom of the cold mass until 4K level is reached. The level in the 4K reservoir is regulated by the LHe supply valve, the level in the 2K phase separator is regulated by the JT valve and the 2K pressure is regulated by the sub-atmospheric line valve. Piping within the module delivers the syphon supply to a number of 4K thermal intercept points (WCT, ICT and FPC) and then returns the two phase LHe back to the top of the 4K phase separator.

Cryogenic System

The design of the cryomodules allows a simplified cryogenics system. A standard commercial 4K cold box is employed delivering 4K liquid to a supply dewar near atmosphere. The LHe in the dewar is pushed through the cold distribution with slight overpressure (1.3Bar) and delivered to the cryomodule 4K reservoir with parallel feed from a common distribution trunk and cold return back from each cryomodule to the exhaust side of the trunk. The distribution has a 'keep cold' return pipe that joins the supply side of the trunk to the return side. Each cryomodule has an associated variable LHe supply

valve. The 4K supply and return operates as a refrigerator load. The sub-atmospheric system is independent from the cold box and operates as a liquefaction load. Each cryomodule is pumped in parallel from a common pump line while a variable valve controls the pressure. A common pump line leads between the cryomodules and the sub-atmospheric pumps in a separate building. A common valve near the sub-atmospheric pumps optimizes the operating pressure at the pumps for a given mass-flow. The return 2K exhaust is warmed passively in a counter flow heat exchanger by thermal exchange with the helium high pressure stream going to the cold box. A simplified schematic of the system is shown in Fig. 5.

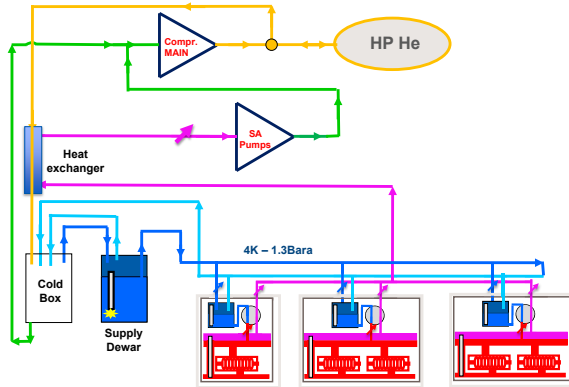


Figure 5: A schematic of the e-Linac cryogenic system.

HLRF System

The rf system includes one high power rf source for each cryomodule. In Phase I each cryomodule will be driven by a dedicated 300kW 1.3GHz klystron. For Phase II one 300kW klystron will drive ACM2 while the ICM will be driven by a 150kW power source to be determined. The ACM rf power feed is split to feed each of the cavities equally. A further splitting is required to feed each of the power couplers while phase shifters in each leg are used to achieve the proper phase conditions. One LLRF system is used for each cryomodule with a vector sum compensation of voltage and phase drifts in the ACM.

STATUS AND COMMISSIONING

Electron Gun

The system is installed and conditioned to 320 kV with beam extracted at 300kV up to the full cw intensity of 10mA. RF modulation of the grid voltage is demonstrated over a wide duty factor range from 0.01% to cw. The transverse emittance of the beam measured with an Allison emittance scanner [6] for a peak current of 10mA and 1% duty factor is $\epsilon_{rms,norm} = 7.5 \mu\text{m}$. This is above the originally specified value of $5 \mu\text{m}$, but still within the acceptance of the planned beamline and accelerator. The bunch length as measured with an rf deflecting cavity in the LEBT analyzing leg at a peak current of 1.75 mA and a grid bias voltage of $U_b = -160 \text{ V}$ is $\pm 12.3^\circ$ with an energy spread of $\Delta E = \pm 500 \text{ eV}$. Estimates based on the

measured transconductance ($g_{21} = 23 \text{ mA/V}$) result in a pulse length of $\phi = \pm 10^\circ$.

LEBT

The LEBT straight section contains three solenoids to provide transverse matching and transportation. A 1.3GHz room temperature buncher provides longitudinal matching to the ICM. A diagnostic line includes a 90° bending spectrometer, diagnostic boxes and a 1.3GHz TM011 mode rf deflector for bunch length measurements. [6] In an initial configuration the LEBT allowed a full 3-D characterizations of the beam phase spaces. The transverse phase space was characterised in a high power Allison scanner capable of accepting beam powers up to 1kW. The longitudinal phase space was mapped into the transverse space using the dispersion in the analysing magnet to map energy spread into the horizontal plane and the vertically deflecting rf device to map time spread into the vertical plane. An example is shown in Fig. 6 where screen images taken downstream of the deflector show manipulation of the longitudinal phase space with the buncher cavity. The LEBT is now installed and commissioned.

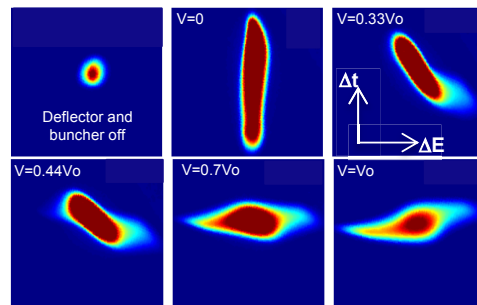


Figure 6: Screen images showing the effective longitudinal emittance as produced by an analysing dipole (ΔE) and rf deflector cavity (Δt). The buncher voltage is varied to manipulate the image.

Cryogenics

The ARIEL cryogenic system [7] includes an ALAT LL Cold Box and KAESER FSD571SFC main compressor with a mass flow rating of 112g/s. In order to arrive at a specification the estimated static loads from the distribution and the cryomodules were multiplied by 1.5 while the active load was doubled assuming that either the Q_0 would be lower by a factor of two or the gradient would be increased to 14 MV/m in some modes. This resulted in a mixed mode set point with a refrigeration load of 128W and a liquefaction load of 220 l/hr (7.6g/s). Considering these requirements a specification of a pure refrigeration performance of 600W and a pure liquefaction performance of 280l/h was defined. The final commissioning produced a pure refrigeration performance of 837W and a pure liquefaction performance of 367l/h comfortably above the criteria. Four Busch Combi DS3010-He sub-atmospheric pumping units rated at 1.4g/s each are installed. More can be added as the 2K production increases in Phase II.

HLRF

Two CPI 290kW cw 1.3GHz klystrons and two 600kW 65kV klystron power supplies from Ampegon are now installed [8]. Each klystron reached the goal specification at the factory. At TRIUMF tests were limited by the available load or circulator – one was operated to 250kW cw the other to 150kW cw. Power couplers are conditioned two couplers at once at room temperature using a 30kW IOT. The couplers are installed on a waveguide box and power is transmitted to a dummy load. Preparation involves extended bakeout (five days) at 100C with N₂ flowing to cover the ceramic. RF conditioning involved both TW (18kW cw) and SW mode (10kW pulsed) with adjustable short for ~five days.

Cavities

The ARIEL cavities have been fabricated by PAVAC. To date three cavities have been received. The cavities are tuned, degreased then given a 120micron BCP before final tuning. After the initial cold test the ARIEL1 and ARIEL2 were each degassed at FNAL at 800C for four hours. Both cavities exhibit similar test results. The cavities reach the specified gradient of 10MV/m but at a Q₀ of 6e9 (see Fig. 9). Since the available cryogenic power is more than enough for Phase I it was decided to accept Q₀>5e9 as a Phase I specification to allow moving forward with the cryo-engineering characterization. ARIEL3 is presently being used to optimize the cavity process. A fourth cavity is due for completion at the end of Sept. 2014. Cavity jacketing is done at PAVAC. Due to problems with Ti-bellows from the sub-contractor PAVAC proposed to machine Ti flexures into the jacket. These work well with no significant increase to the cavity stiffness of 1800N/mm.

Cryomodules

The cryomodule test strategy utilizes the ARIEL1 and ARIEL2 cavities to qualify the two cryomodule types. ARIEL1 is chosen for ICM production while ARIEL2 is chosen for ACM1 installation along with a 'dummy' cavity that occupies the second cavity space in the cryomodule. The dummy cavity contains all the interfaces to the helium system so that all helium piping surrounding the dummy will be final. In addition the dummy cavity is installed with a DC heater to replicate cavity active loads and WPM brackets to permit alignment studies. The one cavity ACM variant we term 'ACMuno'. This configuration allows a full cryo-engineering characterization of the cryomodule. The ICM and ACM preparations each consist of hermetic unit assembly in the clean room, top down assembly in the ISAC beam assembly area and installation in the vacuum tank. The ICM assembly was completed and full cold test was done in the ISAC-II clean room before installation in the e-hall. Due to the size of the ACM it was delivered direct to the e-hall after the top plate was installed and the warm couplers were added there.

10MeV Beam Test

A '10MeV Beam Test' of the front end unit is a project milestone to validate cryogenics, HLRF, LLRF, e-Gun operation, LEPT, ICM engineering and overall synchronization.

Cryogenics characterization: Cooldown to 4K and production of 2K was straightforward. The static heat loads are measured by observing the rate of falling level after the supply valves are closed to the volume and noting the volume change of LHe per unit time and the heat of vapourization. The rate of 2K production is measured by closing the 4K supply valve while regulating the JT valve to keep the level constant in the 2K space. In this case the falling level in the 4K space is a combination of the static loads of the 4K and 2K space plus the vapour lost due to expansion from atmosphere to 31.5mbar. The 77K static load is measured by noting the warmed GN2 flow required at the exhaust side in order to keep the LN2 thermal shield cold. In this case the measurement is an overestimate since it was difficult to regulate the LN2 at a lower level but the thermal shield was always cold. Measured values for the ICM are shown in Table 1 compared to estimates made during the engineering phase. The 2K production efficiency improves as a function of mass flow as the temperature of the heat exchanger and JT valve decreases. Values are 70% at 0.5g/s, 80% at 1g/s and 86% at 1.5g/s.

Table 1: Measured Cryogenics Performance for ICM.

Parameter	Estimate	Measurement
4K static load – no syphon	2W	3W
4K static load with syphon	6W	6.5W
2K static load	5W	5.5W
77K static load	100W	<130W

RF characterization measurements include cavity turn on and phase/amplitude lock, tuner frequency range and tuner lock, microphonics measurements and beam acceleration. The tuner range was measured at +400kHz – the tuner motion was very stable and the cavity frequency could be stepped very precisely over this range. Due to the excellent frequency stability and broad bandwidth phase lock could be obtained with stable forward power even without the tuner but the tuner lock was easily achieved in any case. The spectrum of RF frequency deviation due to microphonics is shown in Fig. 7.

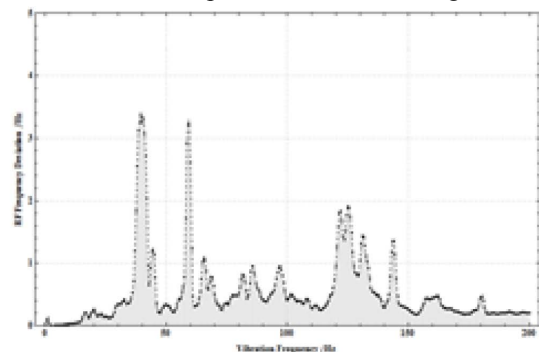


Figure 7: The spectrum of the RF frequency deviation.

The phase error signal in the LLRF phase loop was measured by a spectrum analyser, and was calibrated by modulating the RF reference frequency in closed loop operation. Cavity quality factors were estimated based on calorimetric measurements. The performance is presented in Fig. 8 shown in comparison to the unjacketed vertical test result. The Q_0 values in the cryomodule are equivalent to the values measured in the vertical test indicating the magnetic shielding is sufficient and the HOM dampers do not load the fundamental mode. But the field gradient is restricted due to strong field emission at 5MV/m leading to a repeatable quench at 6MV/m cw. Further tests showed that the 7/9 and 8/9 modes also had quenches near the same values indicating that the problem was most likely in one of the end groups. Cavity conditioning data with a moveable x-ray monitor indicated that the field emission x-rays were most intense on the coupler end of the cavity. As well Cernox sensors on the coupler side beam tube showed some reaction during the quench events.

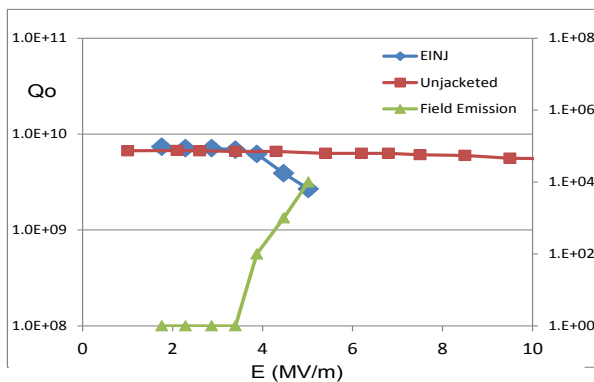


Figure 8: RF characterization of ICM cavity.

Beam Acceleration tests were completed using the MEBT analysing leg as a beam dump. The beam energy was estimated based on the dipole setting at the maximum current intensity into the dump Faraday cup. A low duty factor unbunched beam was first aligned in the LEBT and drifted through the ICM. The ICM cavity was turned on at modest gradient and the phase scanned to achieve a good beam spot on a downstream screen. The analysing leg was then turned on and scanned until the beam was seen on the dump FC. The phase of the cavity was optimized to achieve the maximum energy for the particular cavity gradient while the buncher and optics were used to optimize the transmission. Scans were taken for several cavity gradients and the results are plotted in Fig. 9. Beam simulations were done to calculate the final energy assuming a certain cavity gradient. The expected final energies based on the cavity pick-up signals are plotted and show good agreement.

ICM Recovery: The ICM was taken off-line and the hermetic unit was opened. It was found that the SS damping tube had been scraping on the Nb beam tube causing particulate generation. During assembly when moving from the clean room to the assembly area there was insufficient support for the HOM tube which is

linked to a 77K intercepts and connected to the cavity through a flexible bellows. The cavity was reprocessed,

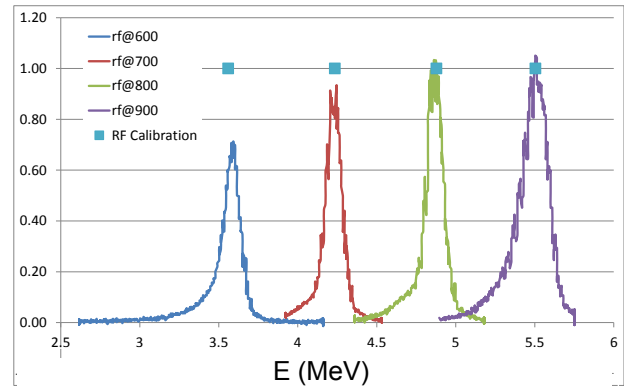


Figure 9: Beam acceleration using ICM compared to expected energy based on rf calibration.

the hermetic assembly parts cleaned and the hermetic unit is being assembled back into the cryomodule for a test in two weeks.

FUTURE PLANS

The ACMuno is now on-line and being cooled down. Beam tests will continue in a few weeks after the recovered ICM is back on line. The beam tests will continue through Dec. 2014 at 25MeV and up to 100kW. In early 2015 a second ICM prepared for VECC in Kolkata will be installed and tested with beam. At the same time ACMuno will be removed and completed with ARIEL4 cavity expected at TRIUMF in the next weeks. The second ACM module is expected for completion in 2018 to complete the e-Linac to its full 50MeV.

REFERENCES

- [1] L. Merminga, et al., "ARIEL: TRIUMF's Rare IsotopE Laboratory", WEOBA001, proc. IPAC 2011.
- [2] W.T. Diamond NIM-A 432 (1999) pp 471-482.
- [3] F. Ames, et al., "The TRIUMF ARIEL RF Modulated Thermionic Electron Source WECF1133, proc. EIC2014.
- [4] P. Kolb, et al., "Cold Tests of HOM Absorber Material for the ARIEL eLINAC at TRIUMF", <http://dx.doi.org/10.1016/j.nima.2013.05.031>.
- [5] R.E. Laxdal, et al., "The Injector Cryomodule for the ARIEL e-Linac at TRIUMF", MOPB091, LINAC12.
- [6] R.E. Laxdal, et al., "TRIUMF/VECC e-Linac Injector Beam test", MOPB026, LINAC12.
- [7] A. Koveshnikov, et al., "Integration and Commissioning of the ARIEL e-Linac Cryogenic System at TRIUMF", ICEC-ICMC2014.
- [8] A. Mitra, et al., Proc. of NA-PAC'13, WEPHO01.